Optimal-Frequency Critical Soft Switching Method of Synchronous DC/DC Converter Based on Model Predictive Control

Liwei Zhou and Matthias Preindl
Department of Electrical Engineering, Columbia University in the City of New York
New York City, NY, USA

Abstract− To improve power density and efficiency, a critical soft switching principle with optimal-frequency model predictive control method is proposed in this paper for DC/DC power converter. Firstly, this paper analyzes the boundary constraints of critical soft switching that are derived with the key parameters of the interlock time and threshold current for typical SiC and GaN devices. Then, according to the derived critical soft switching constraints, two optimal-frequency control methods are proposed based on model predictive control (MPC) to eliminate the turn-on losses especially during the transient period. Compared to the traditional PI controller, the efficiency can be further improved during the reference variation period, because of the fast response of MPC. Finally, the test results verify the theoretical analysis.

I. INTRODUCTION

In power electronics field, SiC and GaN are the two most commonly used devices for the high power density application. To improve the power density of the system, small size of passive devices and high frequency are two main points to be considered when designing the DC/DC converter. [1-2] However due to the large ripple current, the power losses should be paid more attention when reducing the size of inductor. [3] A critical soft switching method with accurate threshold current is proposed in this paper to achieve zero voltage turn-on with pre-designed peak/valley inductor current threshold and dead time. Also, an optimal-frequency critical soft switching control method is proposed based on the MPC. [4-5] Compared to the traditional PI controller, the novel controller can eliminate the turn-on losses especially during the transient period because of the fast response of MPC. [6-9] Thus the critical soft switching operation will be maintained under the variation of reference.

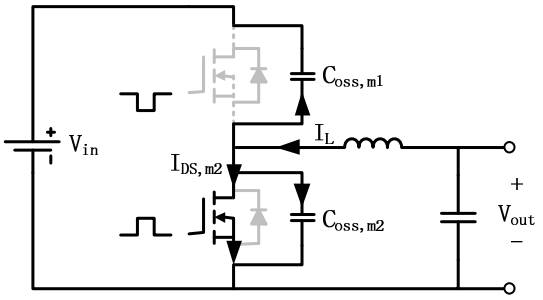

Fig. 1. The negative inductor current paths.

The paper is organized as follow. Firstly, the boundaries of critical soft switching constraints for DC/DC converter are derived with dead time and peak/valley inductor current by data sheet and integral equations. Secondly, the model predictive output voltage and inductor current controller is introduced with the dynamic system parameters which should be updated with the information from the frequency controller. Then, the frequency controller is introduced with two methods according to the requirement of sampling time: one is optimal-frequency control based on the optimization of power losses; another one is maximum-frequency control based on the critical soft switching boundaries. Both of the two methods will receive the duty cycle information from the MPC. Finally, the rigorous test procedures verify the theoretical analysis.

II. CRITICAL SOFT SWITCHING PRINCIPLES FOR DC/DC CONVERTER

In this section, the critical soft switching technique is introduced with the derived boundary conditions of dead time and peak/valley inductor current by datasheet and integral equations. The main purpose of the critical soft switching method is to replace the large turn-on loss of upper switch with small turn-off loss of lower switch.

Fig. 1 shows the current paths of DC/DC converter during lower switch turn-off period. For the critical soft switching, a large current ripple is required to ensure negative valley inductor current to be lower than a threshold current level as is shown in Fig. 2. In the turn-off transient period of lower switch, the negative inductor current will discharge the upper switch output capacitor, $C_{oss,m1}$. The ZVS of upper switch can be achieved if the $C_{oss,m1}$ is fully discharged before it turns on. The ZVS operation depends on the interlock time between two switches and the value of inductor valley current. According to Fig. 1, the inductor valley current can be expressed as:

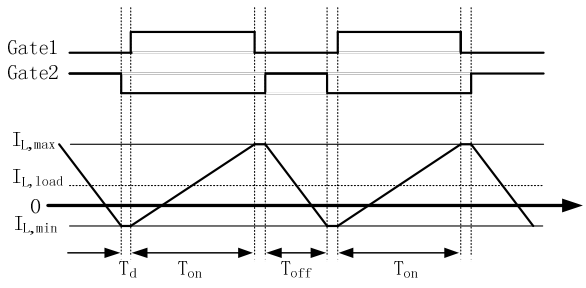

Fig. 2. Gate signals and inductor current for critical soft switching.

$$I_{L,\min} = I_{DS,M2} + I_{\text{coss},M1} + I_{\text{coss},M2} \quad (1)$$

where $I_{DS,M1/2}$ is the drain current, $I_{\text{coss},M1/2}$ is the current through the switch output capacitance, C_{oss}. Because

$$I_{\text{coss},M1(2)} = \mathrm{C}_{\text{oss},M1(2)} \cdot \frac{dU_{DS,M1(2)}}{dt} \quad (2)$$

And ($U_{DS,M1}$+$U_{DS,M2}$) equals to the input source voltage, U_{in}, which is a constant value, then $I_{l,\min}$ can be expressed as:

$$\begin{aligned} I_{L,\min} &= I_{DS,\mathrm{M2}} + (\mathrm{C}_{\text{oss},M1} + \mathrm{C}_{\text{oss},M2}) \cdot \frac{dU_{DS,M2}}{dt} \\ &= I_{DS,\mathrm{M2}} - (\mathrm{C}_{\text{oss},M1} + \mathrm{C}_{\text{oss},M2}) \cdot \frac{dU_{DS,M1}}{dt} \end{aligned} \quad (3)$$

Similarly, the maximum positive value of inductor current is:

$$I_{L,\max} = I_{DS,\mathrm{M1}} + (\mathrm{C}_{\text{oss},M1} + \mathrm{C}_{\text{oss},M2}) \cdot \frac{dU_{DS,M2}}{dt} \quad (4)$$

The above current equations can be further analyzed by the integral calculation over time and U_{ds}, respectively.

$$\begin{aligned} &\int_0^{T_d} \left[I_{L,\min} - I_{DS,\mathrm{M2}}(\mathrm{t}) \right] dt \\ &= \int_0^{U_{in}} \left[\mathrm{C}_{\text{oss},M1}(U_{DS,M2}) + \mathrm{C}_{\text{oss},M2}(U_{DS,M2}) \right] dU_{DS,M2} \\ &\int_0^{T_d} \left[I_{L,\max} - I_{DS,\mathrm{M1}}(\mathrm{t}) \right] dt \\ &= \int_{U_{in}}^{0} \left[\mathrm{C}_{\text{oss},M1}(U_{DS,M2}) + \mathrm{C}_{\text{oss},M2}(U_{DS,M2}) \right] dU_{DS,M2} \end{aligned} \quad (5)$$

For simplification, Ids can be assumed to be varying linearly with time. Then the left side of the above two equations in (5) can be calculated as:

$$\begin{aligned} &\int_0^{T_d} \left[I_{L,\min} - I_{DS,\mathrm{M2}}(\mathrm{t}) \right] dt \\ &= \int_0^{T_d} \left[I_{L,\min} - (I_{L,\min} - \frac{I_{L,\min}}{T_d} t) \right] dt = \frac{1}{2} I_{L,\min} T_d \\ &\int_0^{T_d} \left[I_{L,\max} - I_{DS,\mathrm{M1}}(\mathrm{t}) \right] dt \\ &= \int_0^{T_d} \left[I_{L,\max} - (I_{L,\max} - \frac{I_{L,\max}}{T_d} t) \right] dt = \frac{1}{2} I_{L,\max} T_d \end{aligned} \quad (6)$$

So, the critical soft switching inequalities of $I_{L,\min(\max)}$ and T_d can be expressed as:

$$\begin{aligned} &\frac{1}{2} I_{L,\min} T_d \le \int_0^{U_{in}} \left[\mathrm{C}_{\text{oss},M1}(U_{DS,M2}) + \mathrm{C}_{\text{oss},M2}(U_{DS,M2}) \right] dU_{DS,M2} \\ &\frac{1}{2} I_{L,\max} T_d \ge \int_{U_{in}}^{0} \left[\mathrm{C}_{\text{oss},M1}(U_{DS,M2}) + \mathrm{C}_{\text{oss},M2}(U_{DS,M2}) \right] dU_{DS,M2} \end{aligned} \quad (7)$$

Thus the minimum negative and maximum positive inductor current can be derived with the variables of dead time, Td, and the integration of output capacitors with drain-source voltages. The design of the converter should satisfy the two inequalities to make sure the critical soft switching operation. The integration of switch output capacitance with drain-source voltages can be calculated by the datasheet provided by the manufacturer. Fig. 3 shows the relationship of output capacitance with drain-source voltages under the specific testing condition (T_j=25°C, V_{AC}=25mV, f=1MHz). So the integrations of (7) can be calculated by tracing several discrete voltage intervals multiplied by the corresponding capacitance value and then accumulate together. Because the sum of voltages across switch M1 and M2 are constant and equal to U_{in}, so their integration of output

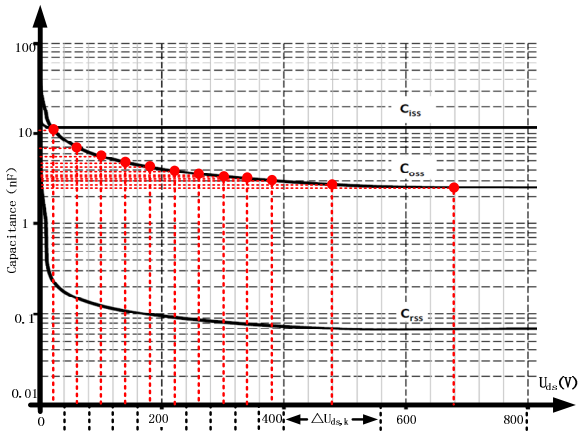

Fig. 3. The traced points of output capacitance with U_{ds}.

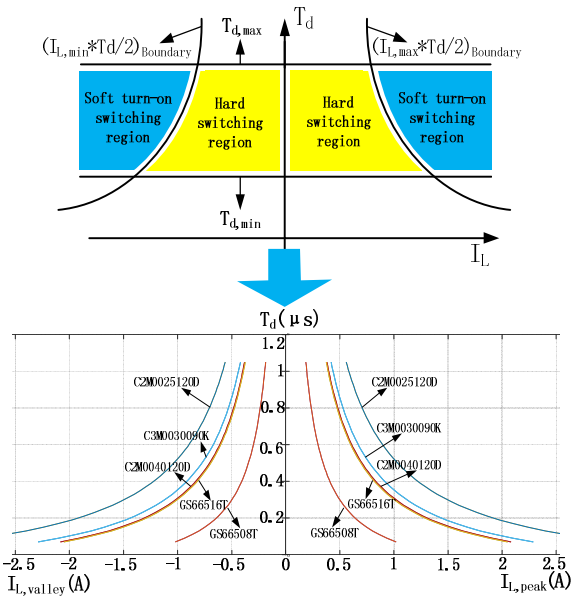

Fig. 4. The soft switching operation regions for different devices.

capacitance with drain-source voltages are identical during the integral limits from 0 to U_{in} and U_{in} to 0, respectively. Then, only one switch integration is needed to be calculated. According to Fig. 3, the right side of (7) can be derived by tracing n points on the curve of C_{oss} and summing up the n intervals together:

$$\begin{aligned} &\int_0^{U_{in}} \left[\mathrm{C}_{\text{oss},M1}(U_{DS,M2}) + \mathrm{C}_{\text{oss},M2}(U_{DS,M2}) \right] dU_{DS,M2} \\ &\approx 2 \sum_{k=1}^{n} \mathrm{C}_{\text{oss},M2}(U_{DS,M2k}) \Delta U_{DS,M2k} \end{aligned} \quad (8)$$

Then, the model of critical soft-switching method can be expressed with the function image in Fig. 4. It can be shown that the blue regions are the feasible soft switching range according to the constraints of (7) with the maximum and minimum dead time requirement. Also, the soft switching ranges of typical GaN and SiC devices are given in Fig. 4. During controlling part in the following sections, the dead time and peak/valley inductor current can be controlled within the critical soft switching region for the converter.

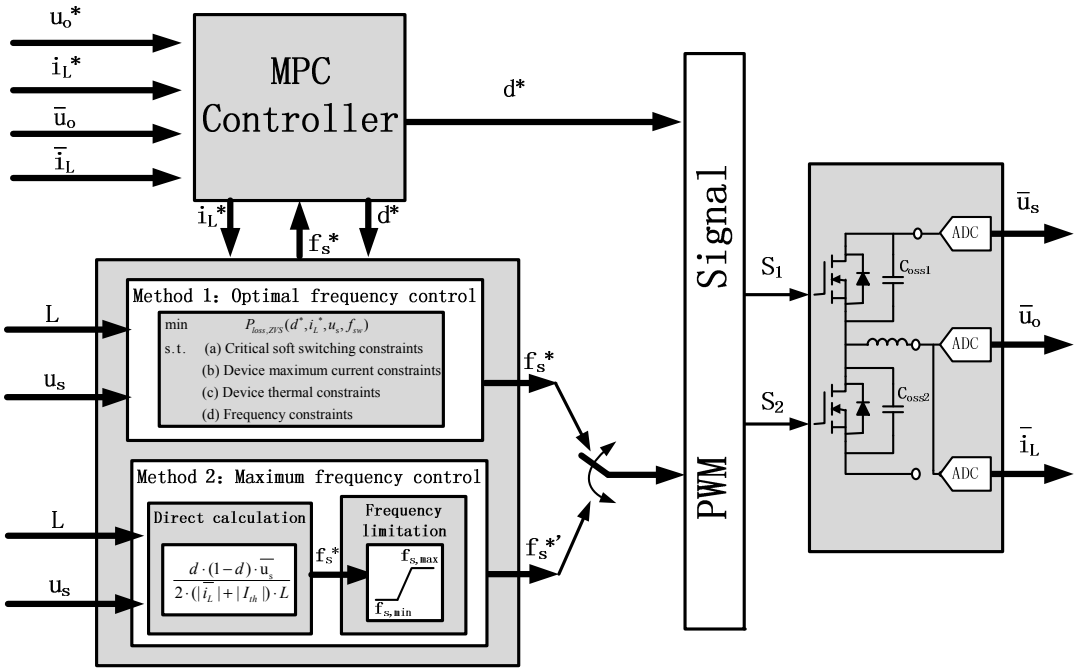

Fig. 5. Controlling blocks.

III. CONTROLLER

The proposed optimal-frequency model predictive controller is introduced in this section. The controller includes two parts: first part is the model predictive voltage and current control; second part is the variable frequency control which can be based on the power loss optimization or critical soft switching boundaries (depend on the required sampling time). In the operating period, the MPC controller will track the output voltage and inductor current references to generate the duty cycle. The duty cycle will be applied for the frequency control based on the power loss optimization or critical soft switching boundaries to generate the optimal frequency. Meanwhile, the optimal frequency will be further applied for the MPC controller to determine the time period of horizon. The controlling blocks are shown in Fig. 5. Following is the detailed analysis.

A. Model Predictive Control for Voltage and Current

The model of the DC/DC converter can be expressed as:

$$\begin{cases} L\dfrac{di_L(t)}{dt} = d(t)\cdot U_{in} - u_{out}(t) \\ C\dfrac{du_{out}(t)}{dt} = i_L(t) - i_{out}(t) \end{cases} \tag{9}$$

To discretize the state equations [10-12]:

$$\begin{cases} i_L(k+1) = i_L(k) - \dfrac{T_s(k)}{L}\cdot u_{out}(k) + \dfrac{U_{in}\cdot T_s(k)}{L}\cdot d(k) \\ u_{out}(k+1) = \dfrac{T_s(k)}{C}\cdot i_L(k) + u_{out}(k) - \dfrac{T_s(k)}{C}\cdot i_o(k) \end{cases} \tag{10}$$

So the state value, X_k, input value, U_k, parametric matrix, A and B for the discrete state equation can be expressed as:

$$\begin{aligned} &X_k = \left[i_L(k) - i_{Lr}(k); u_{out}(k) - u_{or}(k)\right]; \\ &U_k = \left[d(k)\right] \\ &A = \left[1, -\frac{T_s(k)}{L}; \frac{T_s(k)}{C}, 1\right];\ B = \left[\frac{U_{in}\cdot T_s(k)}{L}; 0\right]; \\ &w(k) = \left[0; -\frac{T_s(k)}{C}\cdot i_o(k)\right] \end{aligned} \tag{11}$$

To track the output voltage and inductor current references, the formulation of MPC can finally be expressed as:

$$\begin{aligned} \min\quad & \sum_{k=0}^{N} X_k{}^T Q\, X_k + \sum_{k=0}^{N-1} \Delta U_k{}^T R\, \Delta U_k \\ \text{s.t.}\quad & X_{k+1} = AX_k + BU_k + w_k \in \chi; \\ & \Delta U_k = U_k - U_{k-1}; U_k, U_{k-1} \in \upsilon; \end{aligned} \tag{12}$$

where Q is [q, 0; 0, q] and R is [r] (q and r represent the weight between the two terms in the cost function). It should be noted that, in each sampling instant, the MPC controller generate the duty cycle and receive the optimal frequency value from the frequency controller to update the matrix A and B in (11). [13-15]

B. Variable-Frequency Control for Critical Soft Switching

For the frequency controller, the main purpose is to operate the converter in critical soft switching region and minimize the power losses. In every sampling period, the frequency controller will receive the duty cycle and current reference values from the MPC controller to calculate the optimal frequency. Two methods are provided in this paper according to the sampling time requirement. If the sampling time is long enough, method 1 is applied to optimize the power losses based on Newton iterative method. Otherwise, a more straightforward way, method 2, is also provided to directly calculate the maximum feasible frequency according to the

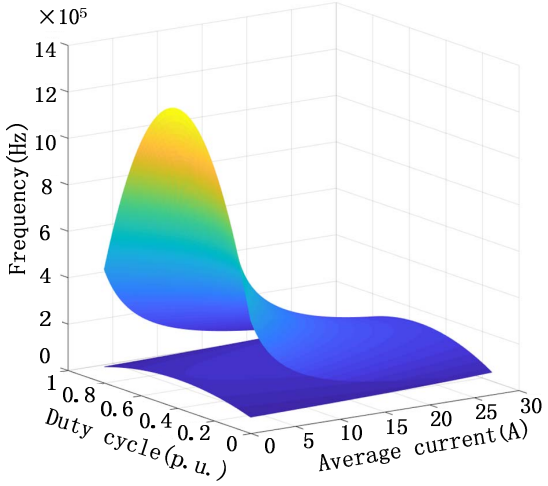

(a)

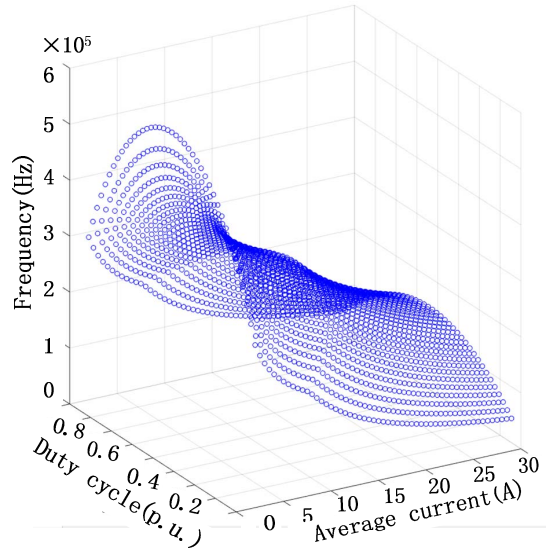

(b)

Fig. 6. The thermal, soft switching, frequency and device current constraints (a) of f_{sw} with the function of duty and I_{ave} (b) the optimal f_{sw} regions with relationship of duty and I_{ave}.

critical soft switching constraints. In this way, the critical soft switching can be guaranteed with high level of frequency. Detailed analysis is as follow.

(1) Method 1: Optimal Frequency Control Based on Power Losses Optimization

The principle of method 1 is to generate the optimal frequency based on the optimization of power losses of the DC/DC converter. As is shown in Fig. 5, the frequency controller receives the information of duty cycle and current reference from the MPC controller. Then the optimization problem is calculated based on the cost function of power losses and four parts of constraints (including: critical soft switching, maximum device current, thermal and sampling requirement).

The power losses cost function under critical soft switching can be expressed as four terms: switch turn-off losses, switch conduction losses, inductor losses and body diode conduction

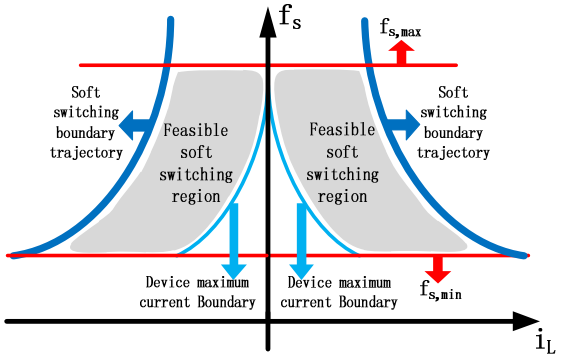

Fig. 7. The feasible regions of MPC method with certain duty.

losses during the dead time:

$$\begin{aligned}&\min \quad P_{off,M}+P_{con}+P_L+P_{con,D}\\&=U_{ds,\max}\cdot I_{ave}\cdot(t_{ru}+t_{fi})\cdot f_{sw}+R_{ON}\cdot\left[I_{ave}{}^2+(\frac{\Delta i_L}{2\sqrt{3}})^2\right]\\&+\left\{K\cdot f_{sw}{}^x\cdot B^y+\left[I_{ave}{}^2+(\frac{\Delta i_L}{2\sqrt{3}})^2\right]\cdot R_{DCR}+(\frac{\Delta i_L}{2\sqrt{3}})^2\cdot R_{ACR}\right\}\\&+u_{sd}\cdot\left[T_{d,D1}\cdot(I_{ave}+\frac{\Delta i_L}{2})+T_{d,D2}\cdot(I_{ave}-\frac{\Delta i_L}{2})\right]\cdot f_{sw}\end{aligned} \tag{13}$$

where the $t_{ru/fi}$, R_{ON}, K, x, y, $R_{DCR/ACR}$, u_{sd}, $T_{d,D1/D2}$ are the inherent parameters: t_{ru} and t_{fi} are the voltage rising time and current falling time during the turn-off period; K, x, y are the core material constants and R_{DCR}, R_{ACR} are the DC and AC equivalent series resistance of the inductor.

The constraints mainly include critical soft switching threshold current, I_{th}, maximum device current, I_{max}, maximum thermal rising, $P_{thermal,max}$ and frequency ranges:

$$\begin{aligned}s.t.\quad &(a)\ I_{th}\le I_{p+}=I_{L,ave}+\frac{\Delta i_L}{2}\le I_{\max};\\&(b)\ -I_{\max}\le I_{n-}=I_{L,ave}-\frac{\Delta i_L}{2}\le -I_{th};\\&(c)\ P_{sw}+P_{con}\le P_{thermal,\max}=\frac{T_{j,\max}-T_{case}}{R_{th,J-C}};\\&(d)\ f_{sw,\min}\le f_{sw}\le f_{sw,\max}\end{aligned} \tag{14}$$

The derived cost function (13) and constraints (14) can both be expressed as the function of the variables, (I_{ave}, d, f_s), after replacing the $\triangle i_L$ with $[(1-d)d*u_s]/(f_s*L)$. So the constraint region and optimal frequency points can be plotted in the 3D axis as is shown in Fig. 6. For the online calculation, according to the Newton Method, by applying the 2nd order Taylor Expansion of the power loss function, the optimal point of frequency can be obtained with the iterative formula of 1st and 2nd power loss derivative in every calculating round:

$$f_{sw,k+1}=f_{sw,k}-\frac{P'_{loss}(f_{sw,k})}{P''_{loss}(f_{sw,k})} \tag{15}$$

The terminating conditions in every calculating round are

the $f_{s,min}$ and $f_{s,max}$ derived from the constraints and the pre-defined error.

(2) Method 2: Maximum Frequency Control Based on Critical Soft Switching Boundaries

For the requirement of faster calculation of frequency, method 2 can be used to directly derive the feasible maximum frequency. The operating trajectories of the frequency controller can be illustrated in Fig. 7. With the variation of current reference, the maximum feasible frequency under the critical soft switching constraints can be derived by the function of frequency and average current (bold blue lines in Fig. 7):

$$f_s = \begin{cases} \dfrac{(1-d)\cdot d\cdot U_s}{2\cdot(\overline{i_L}+I_{th})\cdot L}, & i_L \geq 0 \\ \dfrac{(1-d)\cdot d\cdot U_s}{2\cdot(I_{th}-\overline{i_L})\cdot L}, & i_L \leq 0 \end{cases} \quad (16)$$

where the threshold current of critical soft switching constraints is based on the results derived in section II (7).

For implementing the maximum frequency control method, the peak/valley inductor current will be constrained around the edge of critical soft switching boundaries. Thus the maximum device current requirement will not be violated. As is shown in Fig. 7, the critical soft switching boundary is the exact operating trajectory to follow (bold blue lines). And the device maximum current boundary (fine blue lines in Fig. 7) is another constraint which is far away from the operating bold lines. As is shown in Fig. 5, the maximum and minimum frequency filter is added in the frequency controller to give the upper and lower boundaries of the operating lines according to the sampling and dead time requirement (red straight lines in Fig. 7). Thus, the maximum frequency controller can derive the feasible maximum frequency for the MPC optimization under the critical soft switching operation. And the calculating speed is faster.

IV. RESULTS

The optimal-frequency model predictive control is implemented in this section based on a typical SiC device, C2M0025120D by rigorous testing procedure. The circuit parameters are: input voltage 800V, output voltage 400V, inductor 10uH, operation time 4ms. Fig. 8(a) and (b) show the comparison of the key waveforms between the proposed method and the traditional PI controller with the same current reference step (from 5A to 15A) triggered in the middle of the operating period. Specifically, the inductor current, sampling current, duty cycle and time period are given in each plot. As is shown in Fig. 8(a), the critical soft switching constraints can be satisfied in all the operation time including the transient period. However, the traditional PI controller cannot guarantee the critical soft switching during the transient period because of the oscillation. So the proposed variable-frequency model predictive control method can further reduce the power losses. Also, the test bench of synchronous converter is shown in Fig. 9.

V. CONCLUSION

This paper proposes an optimal frequency critical soft switching method for DC/DC converter based on MPC. The precise critical soft switching boundaries for DC/DC converter are derived with the parameters of dead time and peak/valley inductor threshold current. The MPC is

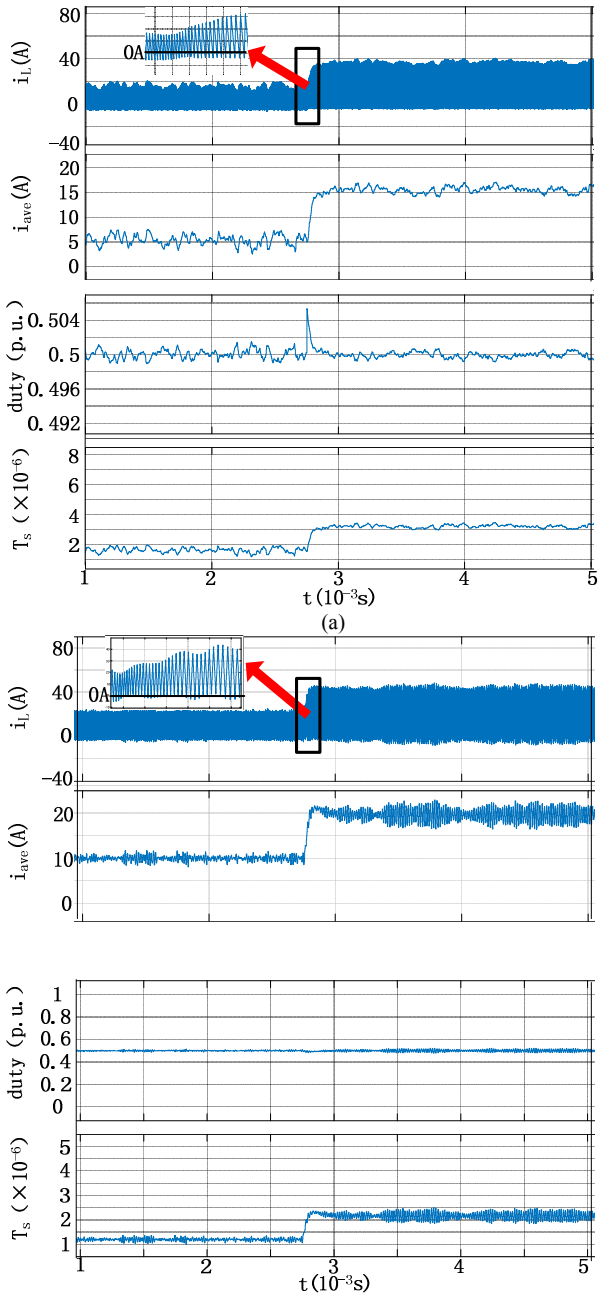

Fig. 8. The key waveforms of inductor current, duty cycle, time period between (a) proposed MPC method and (b) PI.

combined with two types of frequency control methods, optimal-frequency and maximum frequency, to achieve fast response in case of the reference variation. The proposed methods can eliminate turn-on power losses during the transient period which further improves the efficiency compared to the traditional PI controller. The results verify the validity of the theoretical analysis.

VI. ACKNOWLEDGEMENT

This research is based in part upon work supported by National Science Foundation under Grant Number 1653574.

REFERENCES

[1] C. Xiao, G. Chen, and W. G. Odendaal, "Overview of Power Loss Measurement Techniques in Power Electronics Systems," IEEE Transactions on Industry Applications, vol. 43, no. 3, pp. 657–664, 2007.

[2] Y. Rao, S. P. Singh, and T. Kazama, "A Practical Switching Time Model for Synchronous Buck Converters," Proc. IEEE Applied Power Electronics Conference and Exposition, Long Beach, CA, pp. 1585–1590, 2016.

[3] Y. Ren, M. Xu, J. Zhou, and F. C. Lee, "Analytical Loss Model of Power MOSFET," IEEE Transactions on Power Electronics, vol. 21, no. 2, pp. 310–319, 2006.

[4] J. Rodriguez, J. Pontt, C. A. Silva, P. Correa, P. Lezana, P. Cortes, and U. Ammann, "Predictive current control of a voltage source inverter," IEEE Trans. Ind. Electron., vol. 54, p. 495503, 2007.

[5] A. Bemporad, M. Morari, V. Dua, and E. N. Pistikopoulos, "The explicit solution of model predictive control via multiparametric quadratic programming," in ACC, 2000.

[6] M. Preindl, E. Schaltz, and P. Thogersen, "Switching frequency reduction using model predictive direct current control for high-power voltage source inverters," IEEE Trans. Ind. Electron., vol. 58, no. 7, pp. 2826– 2835, 2011.

[7] S. Bolognani, S. Bolognani, L. Peretti, and M. Zigliotto, "Design and implementation of model predictive control for electrical motor drives," IEEE Trans. Ind. Electron., vol. 36, pp. 1925–1936, 2009.

[8] S. Mariethoz and M. Morari, "Explicit model predictive control of a PWM inverter with an LCL filter," IEEE Trans. Ind. Electron., vol. 56, no. 2, pp. 389–399, 2009.

[9] S. Kouro, P. Cortes, R. Vargas, U. Ammann, and J. Rodríguez, "Model predictive control—A simple and powerful method to control power converters," IEEE Trans. Ind. Electron., vol. 56, no. 6, pp. 1826–1838, 2009.

[10] S. Vazquez, C. Montero, C. Bordons, and L. Franquelo, "Model predictive control of a VSI with long prediction horizon," in Proc. 2011 IEEE Int. Symp. Industrial Electronics (ISIE), 2011, pp. 1805–1810.

[11] Z. Song, C. Xia, and T. Liu, "Predictive current control of three-phase grid-connected converters with constant switching frequency for wind energy systems," IEEE Trans. Ind. Electron., vol. 60, no. 6, pp. 2451–2464, 2013.

[12] P. Cortes, J. Rodríguez, D. Quevedo, and C. Silva, "Predictive current control strategy with imposed load current spectrum," IEEE Trans. Power Electron., vol. 23, no. 2, pp. 612– 618, 2008.

[13] S. Kouro, B. La Rocca, P. Cortes, S. Alepuz, B. Wu, and J. Rodríguez, "Predictive control based selective harmonic elimination with low switching frequency for multilevel converters," in Proc. IEEE Energy Conversion Congr. and Expo. (ECCE 2009), pp. 3130–3136.

[14] H. Aggrawal, J. Leon, L. Franquelo, S. Kouro, P. Garg, and J. Rodríguez, "Model predictive control based selective harmonic mitigation technique for multilevel cascaded H-bridge converters," in Proc. 37th Annu. Conf. IEEE Industrial Electronics Society (IECON 2011), pp. 4427–4432.

[15] R. Vargas, P. Cortes, U. Ammann, J. Rodríguez, and J. Pontt, "Predictive control of a three-phase neutral-point-clamped inverter," IEEE Trans. Ind. Electron., vol. 54, no. 5, pp. 2697–2705, 2007.